Postprint of: Bekasiewicz A., Koziel S., Asymmetrical-Slot Antenna with Enhanced Gain for Dual-Band Applications, 2019 13th European Conference on Antennas and Propagation (EuCAP), 31.03-05.04.2019, Krakow, Poland, pp. 1-4

© © 2019 IEEE. Personal use of this material is permitted. Permission from IEEE must be obtained for all other uses, in any current or future media, including reprinting/republishing this material for advertising or promotional purposes, creating new collective works, for resale or redistribution to servers or lists, or reuse of any copyrighted component of this work in other works.

Asymmetrical-Slot Antenna with Enhanced Gain for Dual-Band Applications

Adrian Bekasiewicz[1] and Slawomir Koziel[1,2]

[1] Faculty of Electronics, Telecommunications and Informatics, Gdansk University of Technology, 80-233 Gdansk, Poland
[2] Engineering Optimization & Modeling Center, Reykjavik University, 101 Reykjavik, Iceland

***Abstract*—Dual-band operation is an important feature of antennas to be applied in modern communication systems. Although high gain of radiators is rarely of concern in urban areas with densely located broadcasting stations, it becomes crucial for systems operating in more remote environments. In this work, a dual-band antenna with enhanced bandwidth is proposed. The structure consists of a driven element in the form of an asymmetrical radiator/slot pair suspended over the ground plane. The antenna operates within 2.4 GHz to 3.2 GHz and 4.9 GHz to 6.4 GHz bands with the average gain of 9.7 dBi and 10.4 dBi, respectively. High performance of the structure is achieved through a rigorous two-stage numerical optimization. The antenna lower band covers the industrial, scientific and medical (ISM) radio band which is widely utilized by WiFi, Bluetooth and other systems. The upper band covers all four ranges of the unlicensed national information infrastructure (U-NII) spectrum, applications of which include WiFi 5 GHz, or amateur radio. The proposed structure is compared with other dual-band structures with enhanced gain in terms of size and performance. The effect of the separation between the radiator and ground-plane on the antenna performance is also investigated.**

***Index Terms*—Computer-aided design, design optimization, dual-band antennas, gain maximization, high-gain antennas.**

I. INTRODUCTION

Dual-band antennas are key components of modern wireless communication systems such as WiFi, cellular, long-term evolution (LTE), and others [1]-[3]. Although in urban areas with densely distributed broadcast stations, high antenna gain might not be of primary concern for maintaining high-quality communication, it is one of the most important factors for ensuring accessibility of wireless services in more remote environments. Both the enhanced gain and high directivity can be obtained using antenna arrays [4]-[6]. However, such structures are characterized by relatively large dimensions, which might be a limiting factor for some space-limited and/or indoor applications. From this perspective, availability of radiators providing high-performance at reduced size is of high importance.

Design of dual-band antennas with high-gain is the topic of intensive research. The structures considered in the literature offer improved performance through utilization of resonant cavities [7], [8], dual-loop configurations [9], monopole-based geometries [10], stacked patch radiators [11], [12], slot-based designs [13], [14], and quasi-Yagi topologies [15], [16]. In [7], a microstrip patch antenna with a dual-layer partially reflective surface composed of orthogonal dipole arrays was proposed. Although the structure is characterized by high gain of over 18 dBi and dual-band operation, it offers narrow fractional bandwidths. Moreover, the antenna is characterized by large dimensions of over 150 mm × 150 mm. A more compact, monopole-antenna-based design was proposed in [10]. The structure consists of a fork-shaped radiator enclosed within a rectangular ring and coupled to a rectangular patch radiator. Although the antenna offers a relatively small footprint of 64 mm × 53 mm and competitive fractional gains of 7.5 dBi and 12.5 dBi, it exploits reflective surface located over 100 mm from the radiator which makes it volumetrically large. The antenna of [11] consists of a stack of two patches with U- and I-shaped slots. It features a relatively low profile along with a moderate gain of over 7 dBi. On the other hand, improved performance of the structure is achieved using a large ground plane. Interesting alternative for the considered designs is utilization of slot topologies. In [13], a high-gain antenna based on a slot-radiating element has been proposed. The structure offers relatively broad fractional bandwidths of 44% and 13%, respectively. However, its in-band gain responses are characterized by large variability. Available literature indicates that despite significant differences between the considered antennas, they all exploit reflecting surfaces for gain-enhancement. At the same time, the effect of radiator/reflector distance on the structure performance is not explicitly discussed.

The above considerations indicate that design of dual-band antennas with enhanced gain is a challenging problem where multiple figures related to the structure electrical and field performance as well as size have to be simultaneously accounted for. Due to the lack of theory-based design techniques, the prevailing method for development of such structures is based on manual modifications of topology intertwined with parametric studies and visual inspection of antenna responses [10], [11]. Such a method, however, is insufficient for maintaining reliable control over more than one performance figure at a time (typically the in-band reflection), whereas the remaining ones (including the size, which is mostly affected by the selected antenna topology [17]) are a by-product of the structure topology. Alternatively, the antenna geometry can be described by a curve based on a set of control points, e.g., line sections or splines [18], [19]. The topology of such structure can "evolve" so as to fulfill the prescribed requirements. Typically, this is realized using global optimization methods. However, usefulness of topology-

evolution-based methods to antenna design is limited due to high complexity of the underlying optimization problem and high computational cost associated with global optimization (thousands of EM model evaluations). From this perspective, development of antenna topology based on engineering experience and followed by rigorous local optimization of its performance characteristics seems to be the best available approach for design of dual-band antenna structures with enhanced gain.

In this work, a novel dual-band antenna with enhanced gain is proposed. The structure is based on an asymmetrical slot-radiating element suspended over a reflector surface. High performance of the structure is achieved by means of a two-step optimization where minimization of the in-band reflection is followed by a constrained maximization of gain. The antenna operates within 2.4 GHz to 3.2 GHz and 4.9 GHz to 6.4 GHz bands with the average gain of 9.7 dBi and 10.4 dBi, respectively. The proposed antenna is compared to state-of-the-art radiators from the literature in terms of performance and size. The effects of the vertical separation between the reflector and the radiating element on electrical/field performance are also investigated.

II. High-Gain Dual-Band Antenna

Consider a dual-band antenna shown in Fig. 1. The structure is implemented on a Rogers RO4003C dielectric substrate (ε_r = 3.5, tanδ = 0.0021, h = 0.813 mm). It consists of a driven element in a form an asymmetrical stepped impedance radiator allocated over a stepped width slot. The radiator is fed through a microstrip line with an impedance transformer. The radiator ground plane and the reflector are interconnected through a coaxial feed line. Although the structure is based on a design of [13], it has been substantially modified to increase the number of degrees of freedom and, as a result, improve the control over antenna performance. The changes introduced to the design include removal of the shorted-pin matching circuit, modification of the radiating element through introduction of asymmetrical low-impedance stubs, re-design of the slot to allow for its bi-directional shift w.r.t. the radiator, as well as introduction of the impedance transformer. The antenna geometry is described by a 17-parameter vector $\boldsymbol{x} = [l_1\ l_2\ l_3\ l_{s1}\ l_{s2}\ l_{s3}\ w_1\ w_2\ w_3\ w_{s1}\ w_{s2}\ w_{s3}\ w_{01}\ o\ o_1\ o_2\ l_{01}]^T$, the relative parameters are $A = w_1 + 2l_0 + 2w_0 + 2o$, $B = l_{r1} + l_{r2} + w_0 + 3o$, $l_{r1} = \max(l_1 + l_2, l_{s1} + l_{s2})$ $l_{r2} = \max(l_1 + l_4, l_{s1} + l_{s4})$, $l_{02} = l_{r1} + o - l_{01}$, $l_{03} = w_0 + w_1 + l_0$, whereas dimensions w_0 = 1.75, l_0 = 10, and h_1 = 13 remain fixed (cf. Fig. 1). The unit for all parameters is mm. The antenna model is implemented in CST Microwave Studio and evaluated using its time domain solver. The consistency of structure geometry is maintained for the following lower and upper bounds $\boldsymbol{l} = [9\ 7\ 7\ 7\ 10\ 10\ 1\ 1\ 1\ 1\ 3\ 3\ 3\ 1\ -1\ -1\ 3]^T$ and $\boldsymbol{u} = [17\ 15\ 15\ 12\ 20\ 20\ 5\ 10\ 10\ 5\ 14\ 14\ 5.5\ 7\ 1\ 1\ 10]^T$.

III. Design Methodology

In this section, a brief description of the antenna design methodology is presented. Specifically, we focus on formulation of the design problem along with explanation of the considered optimization strategy. The section is concluded by discussing the optimization algorithm.

A. Problem Formulation and Optimization Strategy

The antenna design problem can be formulated as the following nonlinear minimization task:

$$\boldsymbol{x}^* = \arg\min_{\boldsymbol{x}} U\left(\boldsymbol{R}(\boldsymbol{x})\right) \quad (1)$$

where $\boldsymbol{R}(\boldsymbol{x})$ represents the response of the structure's EM model obtained for a given vector of design parameters $\boldsymbol{x}$; U is the scalar objective function; $\boldsymbol{x}^*$ represents the optimum design to be found.

The antenna design objectives are as follows:

- maximize the gain $\boldsymbol{g}(\boldsymbol{R}(\boldsymbol{x}))$ within 2.4 GHz to 2.5 GHz and 5 GHz to 6 GHz bands;
- maintain the in-band reflection $\boldsymbol{r}(\boldsymbol{R}(\boldsymbol{x}))$ below the –10 dB level.

Due to a poor initial design—resulting from the manual development of the structure topology—direct execution of the optimization process aimed at controlling both objectives at the same time would lead to a poor local optimum that does not fulfill the requirement concerning the acceptable in-band reflection. Therefore, the antenna optimization is executed in a two-step process involving (i) unconstrained minimization of the antenna in-band reflection, and (ii) constrained maximization of the antenna gain. The objective function for the first step is defined as

$$U_1\left(\boldsymbol{R}(\boldsymbol{x})\right) = \max\left(\boldsymbol{r}\left(\boldsymbol{R}(\boldsymbol{x})\right)\right)_{\substack{2.4\text{ GHz to }2.5\text{ GHz}\\5.0\text{ GHz to }6.0\text{ GHz}}} \quad (2)$$

The design obtained from solving (1) with U_1 as the objective function is used as the starting point for the second step. Because evaluation of reflection-related constraint is expensive as it involves simulations of the antenna EM model, here, it is handled implicitly by appropriate definition of the objective function U_2:

$$U_2\left(\boldsymbol{R}(\boldsymbol{x})\right) = -\min\left(\boldsymbol{g}\left(\boldsymbol{R}(\boldsymbol{x})\right)\right)_{\substack{2.4\text{ GHz to }2.5\text{ GHz}\\5.0\text{ GHz to }6.0\text{ GHz}}} + \beta c\left(\boldsymbol{R}(\boldsymbol{x})\right) \quad (3)$$

with

$$c\left(\boldsymbol{R}(\boldsymbol{x})\right) = \left(\frac{\max\{U_1\left(\boldsymbol{R}(\boldsymbol{x})\right) - S_{\max}, 0\}}{S_{\max}}\right)^2 \quad (4)$$

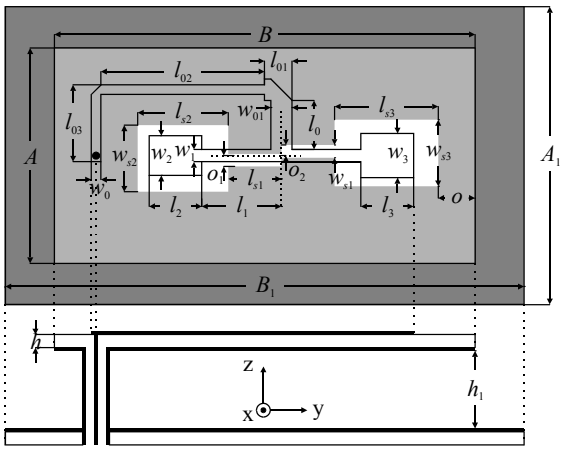

Fig. 1. Top- and cross-section views of the proposed antenna with highlight on its design parameters.

MOST WIEDZY Downloaded from mostwiedzy.pl

The second component contributes to (3) only when the in-band reflection of the antenna is above the specified threshold (here, S_{max} = –10 dB). The penalty factor is set to β = 100 to ensure that contribution of (4) to the objective function U_2 is noticeable beyond acceptable violation of S_{max}.

B. Optimization Algorihtm

The antenna is optimized using a gradient search algorithm embedded in a trust region (TR) framework [20]. The algorithm generates a series of approximations $\boldsymbol{x}^{(i)}$, i = 1, 2, … to $\boldsymbol{x}^*$ by solving

$$\boldsymbol{x}^{(i+1)} = \arg\min_{\boldsymbol{x}:\|\boldsymbol{x}-\boldsymbol{x}^{(i)}\|\le\delta^{(i)}} U\left(\boldsymbol{G}_s^{(i)}(\boldsymbol{x})\right) \quad (5)$$

where $\boldsymbol{G}_s^{(i)}(\boldsymbol{x}) = \boldsymbol{R}(\boldsymbol{x}^{(i)}) + \boldsymbol{J}(\boldsymbol{x}^{(i)})(\boldsymbol{x} - \boldsymbol{x}^{(i)})$ is the first order Taylor expansion model with Jacobian $\boldsymbol{J}(\boldsymbol{x})$ obtained using finite differentiation [21]. The trust region radius δ is iteratively adjusted based on a ratio between the actual and predicted improvement of the objective function

$$\rho = \frac{U_k(\boldsymbol{R}(\boldsymbol{x}^{(i+1)})) - U_k(\boldsymbol{R}(\boldsymbol{x}^{(i)}))}{U_k(\boldsymbol{G}^{(i)}(\boldsymbol{x}^{(i+1)})) - U_k(\boldsymbol{G}^{(i)}(\boldsymbol{x}^{(i)}))} \quad (6)$$

The initial radius is $\delta^{(0)}$ = 1. When $\rho > 0.75$, the radius is updated as $\delta^{(i+1)} = \max(2.5\|\boldsymbol{x}^{(i+1)} - \boldsymbol{x}^{(i)}\|, \delta^{(i)})$, whereas for $\rho < 0.25$ it is decreased as $\delta^{(i+1)} = 0.25\|\boldsymbol{x}^{(i+1)} - \boldsymbol{x}^{(i)}\|$. The candidate design $\boldsymbol{x}^{(i+1)}$ is only accepted if $\rho > 0$. The cost of (5) is N + 1 EM evaluations for successful iterations (with N being the dimensionality of the design problem). More detailed discussion of the algorithm can be found in [20], [21].

IV. Results and Discussion

The starting point for antenna design obtained by the manual topology development is $\boldsymbol{x}_0$ = [11 14 14 7.8 16.2 16.2 2.5 8 8 3.94 10.4 10.4 1.755 0 0 5]^T. The structure has been optimized using the methodology of Section III.*A*. In the first design step, the reflection-oriented antenna optimization has been executed. The design $\boldsymbol{x}_1$ = [14.37 9.15 9.44 10.06 17.13 18.89 1.83 6.85 7.99 1.83 12.57 11.53 3.67 6.5 –0.65 0.45 6.14]^T has been obtained after 8 iterations of (5). The final—gain-optimized—design $\boldsymbol{x}^*$ = [13.12 8.91 8.54 11.33 19.61 19.68 2.72 6.94 7.46 2.64 11.61 13.32 3.6 7 –0.81 0.7 6.52]^T has been obtained after 9 iterations of the TR algorithm. The size of the optimized structure is 80.4 mm × 135 mm × 15 mm. The overall cost of antenna design corresponds to 203 EM model evaluations. A comparison of antenna reflection and gain responses at each stage of the design process is shown in Fig. 2. The optimized antenna features in-band reflection below –10 dB from 2.4 GHz to 3.2 GHz and from 4.9 GHz to 6.4 GHz, respectively, with corresponding average gains of 9.7 dBi and 10.4 dBi. For the frequency ranges defined in the specification (cf. Section III.*A*), the structure maintains the maximum reflection of –10.8 dB and –10.9 dB, as well as the average gains of 10.7 dBi and 11.3 dBi, respectively. It should be noted that enhancement of the lower band for the final design is a by-product of gain-oriented optimization. Figure 4 shows the antenna radiation patterns obtained in the *x*-*z* plane at 2.45 GHz and 5.5 GHz. As expected, the plots indicate directional behavior of the structure with front-to-back ratios of 22.3 dB and 22.9 dB, respectively.

To investigate the effect of radiator/reflector distance (parameter h_1, cf. Section II) on the antenna performance, the structure has been re-designed in a setup with h_1 = 7 mm and h_1 = 19 mm. The results shown in Fig. 4 indicate that vertical separation noticeably affects the field and electrical characteristics of the structure. The best antenna performance has been obtained for h_1 = 13 mm which suggest that it is a close-to-optimal value. Decreasing h_1 results in worsening the antenna average in-band (2.4 GHz to 2.5 GHz and 5 GHz to 6 GHz) gains by 1.8 dB to 2.6 dB, whereas its increase results in gains degradation by 0.6 dB to 1 dB. It should be emphasized that verification of the structure performance for varying radiator/reflector distance is computationally expensive, as it involves re-optimization of all its design variables. Such analyses are normally neglected in the literature, because manual tuning of parameters—which is a prevailing approach for design of novel antennas [10], [11]—is unsuitable for providing conclusive results due to its inability to capture complex mutual relations between variables.

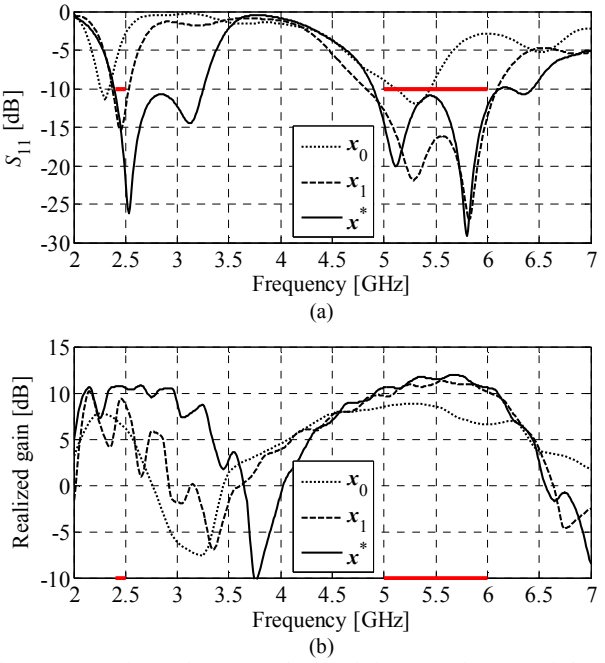

Fig. 2. Comparison of antenna characteristics at each stage of the design process: (a) reflection and (b) realized gain.

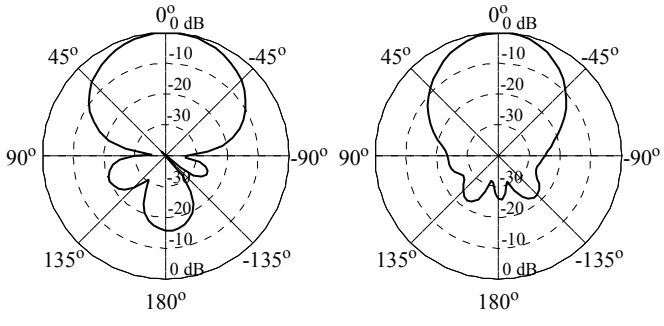

Fig. 3. Radiation pattern characteristics obtained in x-z plane at: (a) 2.45 GHz and (b) 5.5 GHz.

MOST WIEDZY Downloaded from mostwiedzy.pl

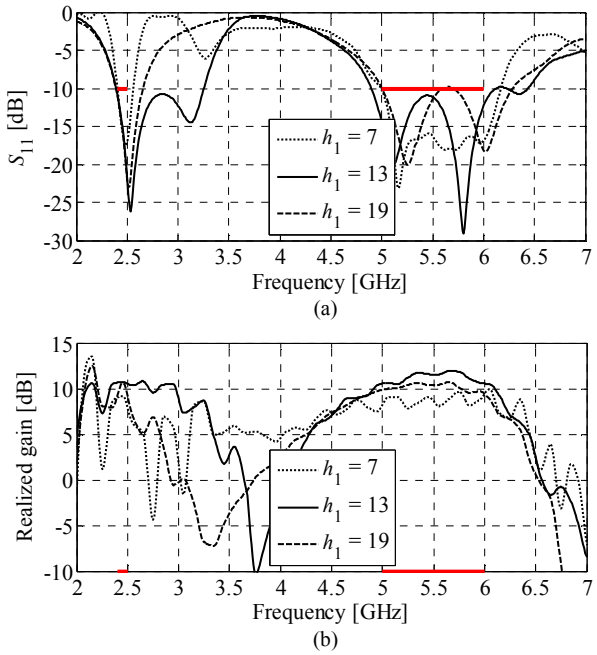

Fig. 4. Effect of radiator/reflector distance on performance of the proposed dual-band antenna: (a) reflection and (b) realized gain.

TABLE I COMPARISON WITH ANTENNAS FROM THE LITERATURE

Design	$f_{0.1}/f_{0.2}$ [GHz]/[GHz]	Bandwidth [%]/[%]	Avg. gain [dBi]/[dBi]	Volume [λ_g^3]
[10]	2.45/5.5	12.6/12.7	5/9.2	0.475
[11]	2.6/3.5	26.9/7.1	7.6/7.1	0.091
[12]	9.73/12.1	4/5.1	14.3/12.5	10.61
[13]	3.0/5.5	44/13	9.4/9.6	0.098
This work	2.8/5.65	30.7/27.1	9.7/10.4	0.129

The proposed antenna has been compared with state-of-the-art structures from the literature in terms of bandwidth, in-band gain and size [10]-[13]. For the sake of fair comparison, fractional bandwidths of considered antennas have been expressed in relation to their center frequencies, whereas antenna dimensions are given in terms of the free-space wavelength (calculated for the lower center frequency). The results shown in Table I indicate that the proposed structure offers competitive performance (w.r.t. both reflection and gain) while featuring acceptable size. At the same time, the antenna outperforms other structures operating at comparable center frequencies in terms of the in-band gain.

V. CONCLUSION

In this work, a novel dual-band antenna with enhanced gain has been proposed. The structure is based on the asymmetrical slot-radiator element suspended over the reflector. Good performance has been achieved as a result of a two-step optimization process oriented towards minimization of the in-band reflection followed by a constrained maximization of gain. The optimized structure features in-band reflection of –10.8 dB and –10.9 dB and average gain of 10.7 dBi and 11.3 dBi within 2.4 GHz to 2.5 GHz and 5 GHz to 6 GHz bands, respectively. The effect of the radiator-to-reflector separation on structure performance has also been investigated indicating its noticeable influence on the structure gain and reflection. The future work will focus on experimental validation of the proposed antenna and its size-reduction-oriented optimization.

ACKNOWLEDGEMENT

The authors thank Dassault Systemes, France, for making CST Microwave Studio available. This work is partially supported by the Icelandic Centre for Research (RANNIS) Grant 174114051, and by National Science Centre of Poland Grant 2017/27/B/ST7/00563.

REFERENCES

[1] G. Li, H. Zhai, Z. Ma, C. Liang, R. Yu, and S. Liu, "Isolation-improved dual-band MIMO antenna array for LTE/WiMAX mobile terminals," *IEEE Ant. Wireless Prop. Lett.*, vol. 13, pp. 1128-1131, 2014.

[2] D. Wang and C.H. Chan, "Multiband antenna for WiFi and WiGig communications," *IEEE Ant. Wireless Prop. Lett.*, vol. 15, pp. 309-312, 2016.

[3] H. Zhai, Q. Gao, C. Liang, R. Yu and S. Liu, "A dual-band high-gain base-station antenna for WLAN and WiMAX applications," *IEEE Ant. Wireless Prop. Lett.*, vol. 13, pp. 876-879, 2014.

[4] Z. Wang, G. Zhang, Y. Yin, and J. Wu, "Design of a dual-band high-gain antenna array for WLAN and WiMAX base station," *IEEE Ant. Wireless Prop. Lett.*, vol. 13, pp. 1721-1724, 2014.

[5] F. Qin *et al*., "A simple low-cost shared-aperture dual-band dual-polarized high-gain antenna for synthetic aperture radars," *IEEE Trans. Ant. Prop.*, vol. 64, no. 7, pp. 2914-2922, 2016.

[6] R.Y. Wu, Y.B. Li, W. Wu, C.B. Shi, and T.J. Cui, "High-gain dual-band transmitarray," *IEEE Trans. Ant. Prop.*, vol. 65, no. 7, pp. 3481-3488, 2017.

[7] H. Moghadas, M. Daneshmand, and P. Mousavi, "A dual-band high-gain resonant cavity antenna with orthogonal polarizations," *IEEE Ant. Wireless Prop. Lett.*, vol. 10, pp. 1220-1223, 2011.

[8] K. Sharma, S. Vaid, and A. Mittal, "Dual-polarized resonant cavity antenna using slotted-circular patch FSS," *IEEE Int. RF Microwave Conf.*, Penang, pp. 75-78, 2013.

[9] S. Su and C. Lee, "Low-cost dual-loop-antenna system for dual-WLAN-band access points," IEEE Trans. Ant. Prop., vol. 59, no. 5, pp. 1652-1659, 2011.

[10] X. He, S. Hong, H. Xiong, Q. Zhang, and E.M.M. Tentzeris, "Design of a novel high-gain dual-band antenna for WLAN applications," *IEEE Ant. Wireless Prop. Lett.*, vol. 8, pp. 798-801, 2009.

[11] S. Liu, W. Wu, and D. Fang, "Single-feed dual-layer dual-band E-shaped and U-slot patch antenna for wireless communication application," *IEEE Ant. Wireless Prop. Lett.*, vol. 15, pp. 468-471, 2016.

[12] B.A. Zeb, N. Nikolic, and K.P. Esselle, "A high-gain dual-band EBG resonator antenna with circular polarization," *IEEE Ant. Wireless Prop. Lett.*, vol. 14, pp. 108-111, 2015.

[13] M. van Rooyen, J.W. Odendaal and J. Joubert, "High-gain directional antenna for WLAN and WiMAX applications," *IEEE Ant. Wireless Prop. Lett.*, vol. 16, pp. 286-289, 2017.

[14] X. Gao, S.M. Li, W.P. Cao, Q. Cheng, H.F. Ma, and T.J. Cui, "A highly directive slot antenna with sidewall corrugated structure," *IEEE Ant. Wireless Prop. Lett.*, vol. 12, pp. 1582-1585, 2013.

[15] H. Liu, Y. Liu, and S. Gong, "A dual-band slot Quasi-yagi antenna with very low profile," *Int. Symp. Ant. Prop.*, Hobart, pp. 1-3, 2015.

[16] M. Awais, H.S. Khaliq, and W.T. Khan, "A novel dual-band millimeter-wave antenna for automotive radar and multi-gigabit wireless communications," *Prog. EM Res. Symp.*, Singapore, pp. 2802-2807, 2017.

[17] S. Koziel and A. Bekasiewicz, "Comprehensive comparison of compact UWB antenna performance by means of multiobjective optimization," *IEEE Trans. Ant. Prop.*, vol. 65, no. 7, pp. 3427-3436, 2017.

[18] M. Ghassemi, M. Bakr and N. Sangary, "Antenna design exploiting adjoint sensitivity-based geometry evolution," *IET Microwaves Ant. Prop.*, vol. 7, no. 4, pp. 268-276, 2013.

[19] L. Lizzi, F. Viani, R. Azaro, and A. Massa, "Optimization of a spline-shaped UWB antenna by PSO," *IEEE Ant. Wireless Prop. Lett.*, pp. 182-185, 2007.

[20] A.R. Conn, N.I.M. Gould, and P.L. Toint, *Trust Region Methods*, MPS-SIAM Series on Optimization, 2000.

[21] S. Koziel and A. Bekasiewicz, "Expedited simulation-driven design optimization of UWB antennas by means of response features," *Int. J. RF Microwave CAE*, vol. 27, no. 6, pp. 1-8, 2017.

MOST WIEDZY Downloaded from mostwiedzy.pl